physica status solidi a
www.pss-a.com

Simultaneous Effect of Ultraviolet Radiation and Surface Modification on the Work Function and Hole Injection Properties of ZnO Thin Films

*Meysam Raoufi, Ulrich Hörmann, Giovanni Ligorio, Jana Hildebrandt, Michael Pätzel, Thorsten Schultz, Lorena Perdigon, Norbert Koch, Emil List-Kratochvil, Stefan Hecht, and Dieter Neher**

The combined effect of ultraviolet (UV) light soaking and self-assembled monolayer deposition on the work function (WF) of thin ZnO layers and on the efficiency of hole injection into the prototypical conjugated polymer poly(3-hexylthiophen-2,5-diyl) (P3HT) is systematically investigated. It is shown that the WF and injection efficiency depend strongly on the history of UV light exposure. Proper treatment of the ZnO layer enables ohmic hole injection into P3HT, demonstrating ZnO as a potential anode material for organic optoelectronic devices. The results also suggest that valid conclusions on the energy-level alignment at the ZnO/organic interfaces may only be drawn if the illumination history is precisely known and controlled. This is inherently problematic when comparing electronic data from ultraviolet photoelectron spectroscopy (UPS) measurements carried out under different or ill-defined illumination conditions.

1. Introduction

Ohmic charge injection into organic semiconductors (OSCs) is crucial for efficient organic optoelectronic devices. Transparent metal oxides are widely used as electron and hole injecting contacts in unipolar and bipolar devices.[1,2] While their high transparency in the visible wavelength range makes them particularly attractive for optoelectronic applications, their high bandgaps allow for selective charge injection and extraction. Among those, zinc oxide (ZnO) is widely used as a hole blocking electrode in electron only devices[3] or as transparent electron-extracting cathode in organic and hybrid solar cells[4,5] Work function (WF) measurements with ultraviolet photoelectron spectroscopy (UPS) typically reveal values of ≈4 eV for untreated ZnO,[6] rendering it an appropriate electrode for n-type organic materials. Self-assembled monolayers (SAMs) based on phosphonic acids (PAs) are frequently employed as interface modifiers to tune the WF of ZnO, enabling efficient injection of electrons and even holes into a wide range of semiconducting molecules and polymers.[7–10] In contrast, ultraviolet (UV) illumination (light-soaking) was shown to lead to transient and persistent changes of the WF of metal oxides, and particularly of ZnO.[11,12] Several studies deal with the influence of the sample environment during UV light soaking on the strength and direction of the WF shift.[13,14] However, there is little work on the interplay between light-soaking and charge injection properties,[13] and the combined effect of light soaking and SAM modification of ZnO has been barely investigated.[15,16] In this work, we use Kelvin Probe (KP) and single carrier device measurements to analyze how the history of light exposure affects the absolute value of the WF and injection properties of unmodified and SAM-modified ZnO films. We find that UV illumination induces a large decrease in the WF of our

M. Raoufi, Dr. U. Hörmann, L. Perdigon, Prof. D. Neher
Institut für Physik und Astronomie
Universität Potsdam
Karl-Liebknecht-Straße 24-25, Potsdam-Golm 14476, Germany
E-mail: neher@uni-potsdam.de

[+]Present address: WI – Leibniz Institut für interaktive Materialien e.V., RWTH Aachen University, Forckenbeckstraße 50, Aachen 52056, Germany; Institut für Technische und Makromolekulare Chemie, RWTH Aachen University, Worringerweg 2, Aachen 52074, Germany

DOI: 10.1002/pssa.201900876

Dr. G. Ligorio, Dr. T. Schultz, Prof. N. Koch, Prof. E. List-Kratochvil
Institute für Physik, Institut für Chemie and IRIS Adlershof
Humboldt-Universität zu Berlin
Brook-Taylor-Straße 6, Berlin 12489, Germany

J. Hildebrandt, Dr. M. Pätzel, Prof. S. Hecht[+]
Institut für Chemie and IRIS Adlershof
Humboldt-Universität zu Berlin
Brook-Taylor-Straße 2, Berlin 12489, Germany

Dr. T. Schultz, Prof. N. Koch
Helmholtz-Zentrum Berlin für Materialien und Energie GmbH
Hahn-Meitner-Platz 1, Berlin 14109, Germany

sol–gel-processed films, independently of whether or not the ZnO surface is functionalized with an SAM. This allowed us to tune the WF over more than 2 eV, and to promote ohmic hole injection into the prototypical OSC poly(3-hexylthiophen-2,5-diyl) (P3HT). Our study also indicates that one monolayer is sufficient to prevent injection barriers due to contact-induced density of states (DOS) broadening.

2. Results and Discussion

Our ZnO samples were prepared via a sol–gel routine in a UV light free environment in ambient atmosphere (see Experimental Section for details of the sample preparation). As shown in **Figure 1**, the WF of such an unmodified ZnO thin film is around 4.65–4.7 eV. This is significantly larger than commonly reported for neat ZnO. High ZnO WFs are generally explained by the adsorption of air-derived acceptors (such as oxygen) at the ZnO surface and at grain boundaries, going along with a reduction of electron density and a concurrent redistribution of charge.[15] We emphasize here that our samples were prepared in the absence of UV light and that the measurement of the WF with KP does not require exposure of the sample to high energy photons (in contrast to commonly used photoelectron spectroscopy techniques). For these samples, the absolute WF of samples could be reproduced within an error of ±80 meV. A WF of 4.4 eV has been previously measured with KP on a layer of ZnO nanoparticles, which was kept in the dark during preparation and measurement.[16] When our ZnO sample is homogenously illuminated with 385 nm UV light (maximum irradiance is ≈35 mW cm^{-2}) for 5 min, the WF exhibits a drastic drop in the WF by nearly 0.8 eV, approaching a value of 3.8 eV which compares well with WF values reported in the literature. We found that 5 min light soaking at this irradiance is sufficient to saturate the WF shift for neat and SAM-modified ZnO (see Figure S1, Supporting Information). Large WF shifts upon UV exposure are commonly attributed to the capture of photogenerated holes by negatively charged oxygen molecules adsorbed at the ZnO surface and at grain boundaries, followed by the desorption of the neutralized entities.[13,16,17]

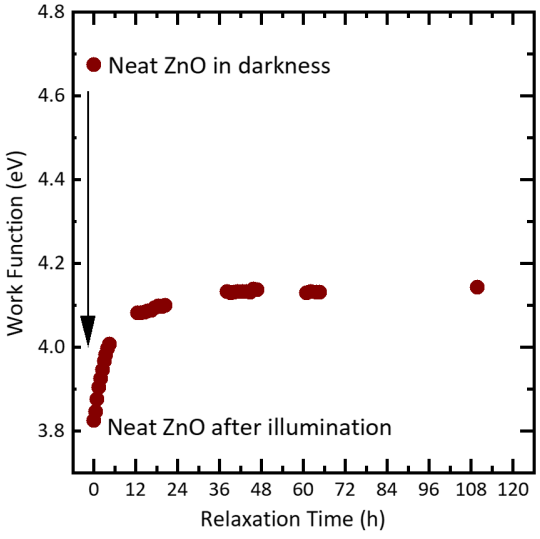

Figure 1. The effect of UV exposure (385 nm) for 5 min in N_2 atmosphere on the WF of neat ZnO, and its subsequent recovery over time in the dark in N_2 atmosphere.

Storing the UV soaked sample in the dark goes along with a partial recovery of the WF, which attains a saturated value of 4.3 eV after ≈48 h. We noticed that the WF never regains the original value of the initial preillumination state, demonstrating the persistent effect of UV soaking. Earlier work reported persistent WF shifts upon UV light exposure of TiO_2 and ZnO if the sample is kept in vacuum or in an inert gas atmosphere.[17,18]

Motivated by this finding, we investigated the effect of the UV radiation on the WF of SAM-treated ZnO. Benzyl phosphonic acid (BPA), 24-fluorobenzyl phosphonic acid, (pyrimidin-2-yl) methylphosphonic acid (PyPA), and BPA:FBPA mixtures were bound to the ZnO surface following a procedure reported previously.[8,9] The open squares in **Figure 2** show the WFs of such treated ZnO substrates, which were prepared and measured in the dark. The SAM modification allows the tuning of the WF over a wide range, from 4.0 to 5.7 eV, depending on the strength and orientation of the SAM dipole moment.

As for neat ZnO, UV soaking causes an abrupt decrease in the WF between 0.5 and 1.0 eV (full circles in Figure 2). As pointed out earlier, the effect of light-soaking on the WF has been explained by the discharge and desorption of air-derived acceptor molecules at the ZnO surface. Herein, we found that UV light soaking decreases the WF regardless of whether the ZnO surface is additionally modified with an SAM. It has been shown that PA molecules, as used in this study undergo tridentate binding to the ZnO surface,[19] meaning that each PA molecule occupies three surface sites. The fact that the presence of the SAM does not reduce the strength of the light-induced WF shift suggests that this phenomenon is not entirely caused by changes of the

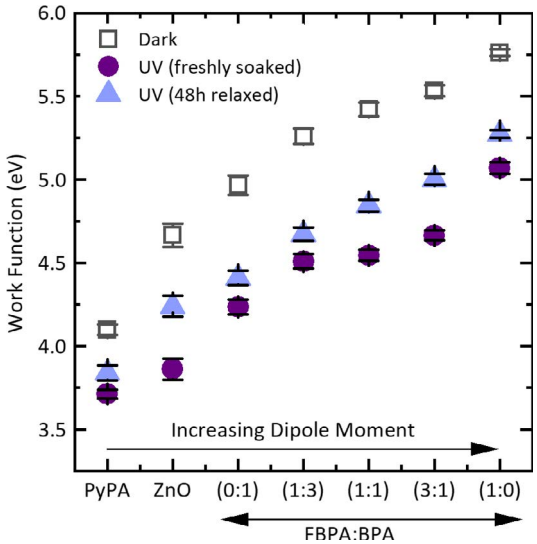

Figure 2. Combined effect of UV soaking and SAM modification on the WF of ZnO. Shown are WF values measured with KP in N_2 atmosphere on substrates prepared and modified in complete darkness (open squares) and the same samples directly after 5 min UV light soaking (closed circles) and after 2 days storage in darkness (closed triangles). The WF of unmodified ZnO is also shown for comparison.

ZnO surface chemistry, but may also involve internal surfaces such as grain boundaries.[11,12,16] As for the bare ZnO, the WF increases again when these UV-soaked ZnO samples are stored in the dark (triangles in Figure 2). Noteworthy, the recovery is smaller for the SAM-treated samples. This is consistent with the results from previous studies on the stability of persistent photoconductivity of neat and SAM-treated ZnO layers in air, where the presence of a dense SAM was proposed to slow down the readsorption of oxygen and other air-derived acceptor molecules by the ZnO surface.[18]

As the shift of the WF upon UV light soaking and/or SAM deposition involves the changes of the ZnO surface composition, it is expected that the strength and, possibly, also the stability of the induced WF shift depends on the particular ZnO preparation route. We have, therefore, performed additional experiments on ZnO layers prepared from nanoparticles (NP-ZnO, see the Experimental Section for further details). Figure S2a, Supporting Information, compares the X-ray photoelectron spectroscopy (XPS) survey spectra of sol–gel ZnO and NP-ZnO films on indium tin oxide (ITO). The overall shape of the spectra is very similar. The detailed analysis of the spectra, however, reveals important differences. For example, the deconvolution of the O1s signal reveals a higher concentration of surface-bound hydroxyl (–OH) groups for the sol–gel-prepared ZnO, whereas the H_2O signal is larger for the NP-ZnO (Figure S2b, Supporting Information).[20,21] Moreover, the bulk phase of the sol–gel ZnO is slightly oxygen deficient compared with the nearly stoichiometric Zn:O ratio of the NP-ZnO. These differences in ZnO composition and surface chemistry may explain the slightly different WFs of the two types of ZnO prior to UV light soaking and/or SAM deposition (Figure S3, Supporting Information). The WF of our freshly prepared NP-ZnO (4.45 eV) agrees very well with the value reported for a similar NP-ZnO layer[16] (see earlier). However, note that the XPS measurements involve the illumination of the sample with X-rays, meaning the results from XPS may not correspond to a "freshly prepared and non-illuminated ZnO layer." UV exposure decreases the WF of both types of ZnO to a similar value of 3.8–3.9 eV. In addition, the subsequent temporal evolution and final value of the WF depends only little on the choice of the ZnO, though we note that the WF decay kinetics is slower for the NP-ZnO sample. We then extended our study to ZnO samples modified by a BPA SAM. Again, while the initial WF is slightly higher for the sol–gel ZnO, the overall evolution of the WF upon UV-illumination and subsequent storage in the dark is comparable for both ZnO films (Figure S4, Supporting Information). This suggests that our conclusions about the strengths of the UV and/or SAM-induced WF shifts and its impact on the injection properties (see later) is representative of thin-film ZnO layers, irrespective of the exact preparation route and surface composition.

According to Figure 2, combining UV soaking with SAM treatment allowed us to tune the absolute WF by ≈2 eV, from 3.7 (for the relaxed UV-treated PyPA sample) to 5.8 eV (the FBPA sample prior to UV illumination). With that, the WF of our samples covers the range of typical hole-injecting anodes. This motivated the question whether such ZnO films may act as efficient hole-injecting contacts, and how the injection efficiency correlates with the ZnO WF. To this end, we prepared hole only devices comprising P3HT, a prototypical hole-transporting OSCs. The sample consisted of a 300 nm thick layer of P3HT, coated from chlorobenzene, sandwiched between the (modified) ZnO bottom contact on a fully covered ITO substrate and circular MoO_3/Al top electrodes (see the Experimental Section and Figure S5, Supporting Information, for details). **Figure 3** shows the results of hole-current measurements for the differently modified ZnO electrodes, which either have never been exposed to UV light (Figure 3a) or underwent 5 min UV exposure followed by 48 h storage in the dark before being overcoated by the P3HT semiconductor (Figure 3b). As expected, the hole only current with injection from MoO_3 (positive bias) is neither affected by the choice of the SAM nor by light soaking. The WF of MoO_3 is significantly higher than the ionization energy of P3HT, promoting the formation of an ohmic contact at this interface. The lower current for the device with a PyPA-treated

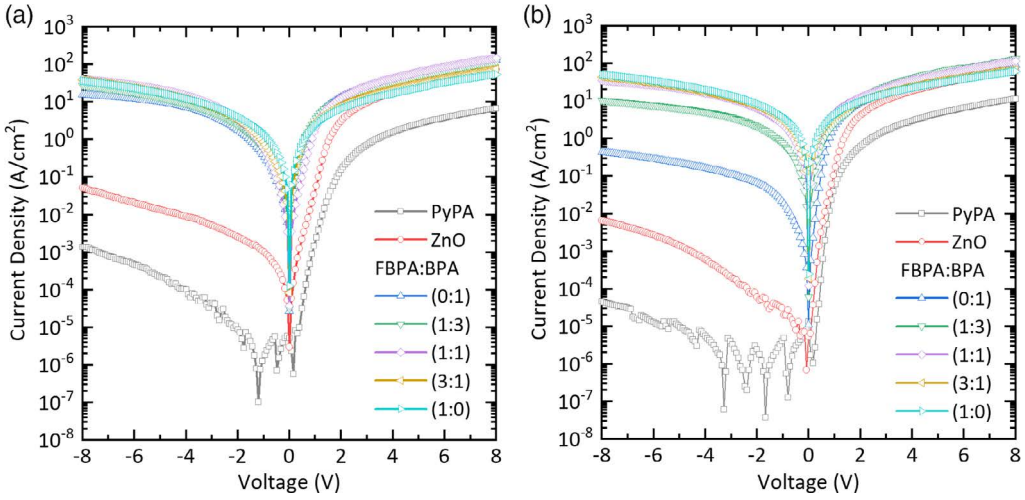

Figure 3. Semilogarithmic *J–V* plot of hole only devices with a ZnO/SAM/P3HT/MoO_3/Ag structure, where the electrode is either bare ZnO or ZnO modified with different SAMs. Data are shown for ZnO films that a) were prepared in complete darkness or b) underwent a 5 min UV soaking followed by 48 h in N_2 atmosphere. A negative bias corresponds to hole injection from the ZnO and a positive bias to hole injection from MoO_3.

SAM is attributed to the fact that these devices were fabricated in a later stage of the project, using a new batch of P3HT. For ohmic injection, the hole only current depends sensitively on the packing, orientation, and mesoscale morphology of the polymer layer in the bulk, which is closely linked to the characteristic properties of the polymer backbone.[22]

If holes are injected from ZnO (negative bias), the introduction of the SAM has a large effect on the hole injection current. For example, the hole injection current for untreated ZnO differs by three orders of magnitude between reverse bias (injection through ZnO contact) and forward bias (injection through MoO_3 contact). This is a clear indication for a significant injection barrier at the ZnO/P3HT interface. Fortunately, the choice of the P3HT batch did only weakly affect the hole injection properties from ZnO at high reverse bias, as detailed in Figure S6, Supporting Information. Increasing the ZnO WF using different SAMs reduces the barrier height and the hole only current approaches the bulk-limited current value under forward bias.

Notably, if the ZnO has never been exposed to UV light, the hole injection current in reverse bias is nearly identical for (FBPA:BPA) 0:1-, 1:3-, 1:1-, 3:1-, and 1:0-modified samples (Figure 3a). This indicates that the Fermi level (E_F) of the modified ZnO substrate is pinned at the highest occupied molecular orbital (HOMO) of the P3HT semiconductor, and the contact is ohmic. In contrast, decreasing the ZnO WF using a PyPA SAM goes along with a significant deterioration of the hole-injecting properties, with the hole injection current decreasing by about two orders of magnitude as compared with the untreated ZnO. Figure 3b shows the corresponding J–V curves for ZnO which was stored in the dark under N_2 atmosphere for 48 h after UV exposure and before P3HT deposition. The data reproduce the trend shown in Figure 3a, but with important differences. Overall, hole injection from SAM-treated and untreated ZnO becomes less efficient after UV exposure, consistent with the reduction of the WF as reported earlier. Meanwhile, for modified samples with high initial WF (here: (FBPA:BPA) 1:1, 3:1, and 1:0) UV soaking does not produce a major effect, as the ZnO Fermi level remains pinned. For these samples, UV exposure causes a slight increase in the current at high reverse bias, which may be caused by an increase in the electrical conductivity of the ZnO due to photodoping.[18]

The results from the different measurements are shown in **Figure 4**, which displays the hole injection current at a reverse bias of −8 V (hole injection from the ZnO bottom electrode) as function of the ZnO WF (WF averages and error bars are from measurements on at least 10 individual devices). As an important conclusion, we find that the hole injection current from SAM-treated ZnO is a sole function of the WF, independent of whether a given WF has been attained by the use of a specific SAM, a specific illumination history, or the combination of both. Two regimes can be identified. For low WF, the contact is non-ohmic and the hole injection current is a strong (exponential) function of the barrier height. In contrast, when the electrode E_F is within or approaches the respective transport band of the semiconductor, thermally induced charge transfer takes place, which pins the substrate E_F at an energy near the onset of the DOS distribution.[2,23,24] In this case, the hole injection current remains constant even if the electrode WF exceeds the ionization energy of OSCs.[19,25] This is well shown in Figure 4, where the hole injection current becomes independent of the ZnO WF above

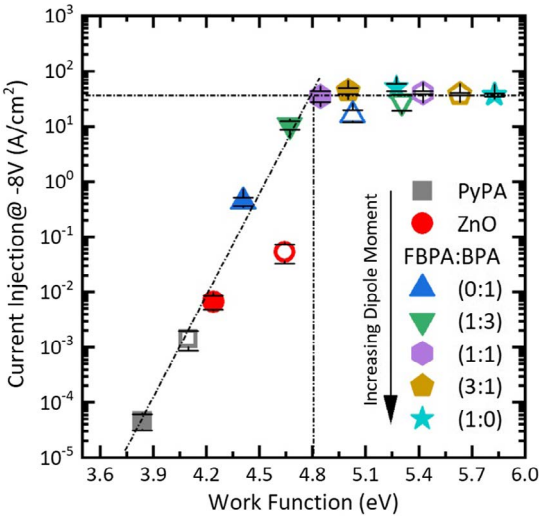

Figure 4. Hole injection from ZnO into P3HT versus the ZnO WF for differently treated ZnO. Open symbols are for ZnO samples prepared in the absence of UV light, whereas closed symbols refer to UV-light-soaked samples.

4.8 eV, which is close to P3HT ionization energy.[26] Surprisingly, hole injection from untreated ZnO (prepared in the dark) is inefficient, despite its fairly high WF of 4.7 eV. It has been proposed that the electrostatic interaction between a metal oxide and an OSC gives rise to a significant broadening of the DOS near the hybrid interface, which reduces the efficiency of charge injection.[1] This was rationalized by a significant broadening of the HOMO near the metal oxide surface. As a consequence, the Fermi level of the metal oxide electrode gets pinned by the deep tail states of the broadened DOS, meaning that the injected charges have to overcome an energetic barrier to enter the bulk of the organic hole transport layer (HTL). Following this rationale, this effect was largely reduced when an interlayer with a deeper lying HOMO was inserted between the metal oxide and the organic HTL. Notably, the UV soaked (FBPA:BPA) 1:3-treated ZnO substrate, which has a very similar WF to untreated ZnO, allows for nearly ohmic injection. We propose that the insertion of the SAM reduces the electrostatic interaction between the ZnO and the OSCs and presumably reduces injection barriers induced by DOS broadening. However, we acknowledge that the injection efficiency may also be affected by differences in the chemical and electronic structure of the neat (non-UV-soaked) and SAM-treated (and UV-soaked) ZnO.

3. Conclusions

In conclusion, we have systematically investigated the combined effect of UV light soaking and SAM surface treatment on the WF and the hole injection properties of thin ZnO films into the prototypical OSC P3HT. We demonstrated ohmic hole injection from SAM-modified ZnO into P3HT, which we attribute to an increased ZnO WF in combination with a reduced electrostatic interaction between the ZnO surface and the OSCs near the hybrid interface. We also documented a drastic effect of UV light soaking on the WF and injection efficiency, meaning that

conclusions regarding the contact properties and barrier heights can be drawn only with the precise knowledge of the preparation and illumination history of the ZnO substrate.

4. Experimental Section

Materials: Zinc acetate and ZnO nanoparticle solutions were purchased from Sigma Aldrich and Avantama N-10, respectively. BPA (97%) and 4-fluorobenzylphosphonic acid (99%) were obtained from Sigma Aldrich and used without further purification. PyPA was synthesized via alkylation of triethyl phosphite as reported earlier.[27] P3HT was purchased from Rieke Metals.

ZnO Layer Preparation: The sol–gel ZnO films were prepared via spin coating from a solution of 100 mg zinc acetate dihydrate in 1 mL of 2-methoxyethanol with 27.7 µL ethanolamine, filtered through a 0.45 µm PTFE filter, at 4000 rpm onto ITO-covered glass slides. This was followed by subsequent annealing at 200 °C for 1 h in air. The NP-ZnO films were prepared via spin coating the ZnO nanoparticle dispersion dispersed in isopropanol through a 0.45 µm PTFE filter at 5000 rpm, followed by thermal annealing at 120 °C for 30 min in air. The film preparation was done under yellow light room lighting in ambient atmosphere. The finished ZnO layers were stored in a N_2-filled glovebox in the dark before usage.

SAM Formation: The PAs for SAM formation were dissolved in dry tetrahydrofuran with the concentration of 1×10^{-3} M. ZnO-covered substrates were immersed into the SAM-containing solution on a hot plate at 40 °C in a covered glass vessel for 1 h. Finally, the SAM-treated samples were dried at 90 °C for 3 min on a hot plate. All preparation steps were performed in a dark N_2-purged glovebox (in a lab with yellow light room lighting).

UV Light Soaking: The ZnO sample was illuminated by a high-power LED with 385 nm UV light (maximum irradiance is ≈35 mW cm^{-2}) homogenously for 5 min in an otherwise dark N_2-purged glovebox.

Kelvin Probe: WFs were measured in a N_2-filled glovebox at room temperature with a KP Technology SKP5050 KP. Note that the KP setup was housed in a metal box, which reduced the electromagnetic noise but also protected the setup and the sample from light. Calibration of the tip WF was done against freshly cleaved, highly ordered pyrolytic graphite (HOPG), for which we assumed a WF of 4.6 eV. WF values and errors in Figure 2 of the main document are from measurements on several independent samples.

X-Ray Photoelectron Spectroscopy: The XPS measurements were conducted in UHV (10^{-9} mbar), using the Mg anode ($K_\alpha = 1253.6$ eV) of a DAR400 X-ray source from Omicron for excitation and an Omicron 75 hemispherical analyzer for the detection of the emitted photoelectrons. Survey spectra were recorded with a pass energy of 50 eV and narrow scans with a pass energy of 20 eV. Sensitivity factors of 12.84 for the Zn $2p_{3/2}$ core level and 2.66 for the O 1s core level were used for quantification.

Single carrier devices: P3HT was dissolved in chlorobenzene at a concentration of 50 mg mL^{-1}. P3HT films were prepared by spin coating from hot (70 °C) solution onto the (SAM-modified) ZnO substrates in a N_2-filled glovebox. The final P3HT layer thickness was about 300 nm. Subsequently, circular MoO_3/Ag (13 nm/200 nm) electrodes with an area of 4.5 mm^2 were thermally deposited as top electrode to complete the device (see Figure S4, Supporting Information). The current–voltage characteristics of these devices were recorded in a N_2-filled glovebox at room temperature, using a Keithley 2400 source meter. For the measurements, P3HT film was carefully removed at one edge for better contacting of the substrate electrode. This area was coated with silver conductive paint. Contact to the top electrodes was done with gold wire with a spherical head to avoid electrode damaging.

Supporting Information

Supporting Information is available from the Wiley Online Library or from the author.

Acknowledgements

This work was funded by the Deutsche Forschungsgemeinschaft (DFG)—Projektnummer 182087777—SFB 951 (HIOS).

Conflict of Interest

The authors declare no conflict of interest.

Keywords

charge injection across hybrid interfaces, energy-level alignments, hybrid metal oxides/organic interfaces

Received: October 22, 2019
Revised: December 18, 2019
Published online: January 29, 2020

[1] N. B. Kotadiya, H. Lu, A. Mondal, Y. Ie, D. Andrienko, P. W. M. Blom, G. J. A. H. Wetzelaer, *Nat. Mater.* **2018**, *17*, 329.
[2] M. T. Greiner, M. G. Helander, W. M. Tang, Z. Bin Wang, J. Qiu, Z. H. Lu, *Nat. Mater.* **2012**, *11*, 76.
[3] M. A. Muth, W. Mitchell, S. Tierney, T. A. Lada, X. Xue, H. Richter, M. Carrasco-Orozco, M. Thelakkat, *Nanotechnology* **2013**, *24*, 484001.
[4] M. S. White, D. C. Olson, S. E. Shaheen, N. Kopidakis, D. S. Ginley, *Appl. Phys. Lett.* **2006**, *89*, 143517.
[5] C. Thu, P. Ehrenreich, K. K. Wong, E. Zimmermann, J. Dorman, W. Wang, A. Fakharuddin, M. Putnik, C. Drivas, A. Koutsoubelitis, M. Vasilopoulou, L. C. Palilis, S. Kennou, J. Kalb, T. Pfadler, L. Schmidt-Mende, *Sci. Rep.* **2018**, *8*, 3559.
[6] R. Schlesinger, F. Bianchi, S. Blumstengel, C. Christodoulou, R. Ovsyannikov, B. Kobin, K. Moudgil, S. Barlow, S. Hecht, S. R. Marder, F. Henneberger, N. Koch, *Nat. Commun.* **2015**, *6*, 6754.
[7] S. A. Paniagua, A. J. Giordano, O. L. Smith, S. Barlow, H. Li, N. R. Armstrong, J. E. Pemberton, J. L. Brédas, D. Ginger, S. R. Marder, *Chem. Rev.* **2016**, *116*, 7117.
[8] Q. Wang, G. Ligorio, V. Diez-Cabanes, D. Cornil, B. Kobin, J. Hildebrandt, M. V. Nardi, M. Timpel, S. Hecht, J. Cornil, E. J. W. List-Kratochvil, N. Koch, *Adv. Funct. Mater.* **2018**, *28*, 1800716.
[9] S. Gutmann, M. A. Wolak, M. Conrad, M. M. Beerbom, R. Schlaf, *J. Appl. Phys.* **2010**, *107*, 103705.
[10] U. Hörmann, S. Zeiske, F. Piersimoni, L. Hoffmann, R. Schlesinger, N. Koch, T. Riedl, D. Andrienko, D. Neher, *Phys. Rev. B* **2018**, *98*, 155312.
[11] A. T. Vai, V. L. Kuznetsov, J. R. Dilworth, P. P. Edwards, *J. Mater. Chem. C* **2014**, *2*, 9643.
[12] Q. Bao, X. Liu, Y. Xia, F. Gao, L. D. Kauffmann, O. Margeat, J. Ackermann, M. Fahlman, *J. Mater. Chem. A* **2014**, *2*, 17676.
[13] S. R. Bobbara, E. Salim, R. Barille, J. M. Nunzi, *J. Phys. Chem. C* **2018**, *122*, 23506.
[14] S. R. Cowan, P. Schulz, A. J. Giordano, A. Garcia, B. A. Macleod, S. R. Marder, A. Kahn, D. S. Ginley, E. L. Ratcliff, D. C. Olson, *Adv. Funct. Mater.* **2014**, *24*, 4671.
[15] M. Madel, F. Huber, R. Mueller, B. Amann, M. Dickel, Y. Xie, K. Thonke, *J. Appl. Phys.* **2017**, *121*, 124301.
[16] G. Lakhwani, R. F. H. Roijmans, A. J. Kronemeijer, J. Gilot, R. A. J. Janssen, S. C. J. Meskers, *J. Phys. Chem. C* **2010**, *114*, 14804.
[17] S. Trost, A. Behrendt, T. Becker, A. Polywka, P. Görrn, T. Riedl, *Adv. Energy Mater.* **2015**, *5*, 1500277.
[18] A. R. McNeill, A. R. Hyndman, R. J. Reeves, A. J. Downard, M. W. Allen, *ACS Appl. Mater. Interfaces* **2016**, *8*, 31392.

[19] C. Wood, H. Li, P. Winget, J. L. Brédas, *J. Phys. Chem. C* **2012**, *116*, 19125.
[20] R.-D. Sun, A. Nakajima, A. Fujishima, T. Watanabe, K. Hashimoto, *J. Phys. Chem. B* **2001**, *105*, 1984.
[21] I. Lange, S. Reiter, J. Kniepert, F. Piersimoni, M. Pätzel, J. Hildebrandt, T. Brenner, S. Hecht, D. Neher, *Appl. Phys. Lett.* **2015**, *106*, 113302.
[22] R. Steyrleuthner, R. Di Pietro, B. A. Collins, F. Polzer, S. Himmelberger, M. Schubert, Z. Chen, S. Zhang, A. Salleo, H. Ade, A. Facchetti, D. Neher, *J. Am. Chem. Soc.* **2014**, *136*, 4245.
[23] C. Tengstedt, W. Osikowicz, W. R. Salaneck, I. D. Parker, C. H. Hsu, M. Fahlman, *Appl. Phys. Lett.* **2006**, *88*, 053502.
[24] M. Oehzelt, N. Koch, G. Heimel, *Nat. Commun.* **2014**, *5*, 4174.
[25] J. C. Hsu, Y. H. Lin, P. W. Wang, Y. Y. Chen, *Appl. Opt.* **2012**, *51*, 1209.
[26] Z. L. Guan, J. B. Kim, H. Wang, C. Jaye, D. A. Fischer, Y. L. Loo, A. Kahn, *Org. Electron.* **2010**, *11*, 1779.
[27] I. Lange, S. Reiter, M. Pätzel, A. Zykov, A. Nefedov, J. Hildebrandt, S. Hecht, S. Kowarik, C. Wöll, G. Heimel, D. Neher, *Adv. Funct. Mater.* **2014**, *24*, 7014.
[28] S. Braun, W. R. Salaneck, M. Fahlman, *Adv. Mater.* **2009**, *21*, 1450.